

Enhanced Antibacterial Activity of Curcumin by Combination with Polyurethane Micelles

Shaomin Song^{*,#}, Meihui Yin[#], Xiaohui Wan, Daoping Yan, Min Yang, Lijiao Yang, Jicong Deng^{*}

Abstract— In recent years, the problem of bacterial resistance has become more and more serious. Drug-resistant strains pose a great threat to human health. Infection mortality and corresponding treatment costs have increased, causing a huge social and economic burden. The study found that curcumin (CUR) can inhibit the growth of bacteria such as *Escherichia coli* and *Staphylococcus*. In order to develop a new type of antibacterial material to treat bacterial infections, this subject designed and synthesized a curcumin polyurethane micelle (MPEG-CUR-PU). The micelles showed a pH responsive transition from a negative charge to a positive charge, while strongly adhering quickly to negatively charged bacterial surfaces at infectious sites (pH = 5.5) based on electrostatic attraction. MPEG-CUR-PU has a good selectivity for bacteria, which makes it a promising antibacterial nanodrug in biomedical field.

Index Terms— Curcumin, Polyurethane micelles, Drug resistance, Targeting, Antibacterial.

I. INTRODUCTION

Bacterial infections have been demonstrating major virulence with a high rate of pathogenicity and mortality for a long time. Bacterial infection will seriously damage human health and affect people's daily life. Some pathogenic bacteria can enter human blood through infection and produce harmful substances and a large number of metabolites, which will cause human infection. Since their introduction in the 1930s, antibiotics have been heralded as the miracle discovery of the 20th century[1-2]. Therefore, the emergence of antibiotics has made a great contribution to medical treatment. Unfortunately, frequent and excessive use of conventional antibiotics has caused extensive multidrug resistance in bacterial infections [3]. Therefore, it is urgent to develop new and effective agents[4]. If nothing changes in the existing trend, it has been predicted that by 2050

antimicrobial resistance (AMR) will be a bigger killer than diseases such as cancer[5]. In the process of treatment, the discovery and use of antibiotics is an important milestone in the history of human anti infection[6]. At present, the two main strategies to solve this crisis are to limit the use of antibiotics and develop new antibiotics[7, 8].

Curcumin (CUR) is a yellow, water-insoluble pigment extracted from root of turmeric[9], a commonly used spice and food-coloring agent in Southeast Asian cooking. In recent years, its anti-inflammatory, anti-oxidation and anti-cancer functions have been widely studied. According to reports, it also has good antibacterial and antifungal properties[10, 11]. They can inhibit the growth and reproduction of bacteria[12], destroy the integrity of cell wall, and interact with different molecular targets in the body[13, 14], which can play an important role in bacterial mediated infectious diseases. When combining with nanotechnology CUR can improve the solubility and bioavailability of drugs. Poonam has studied that CUR can increase the membrane permeability of *E.coli* and *S.aureus* by changing the environment inside and outside the cell, so as to make more drugs enter the cell and play a bactericidal role[15]. CUR can prevent the aggregation of some inflammatory cells, reduce the overexpression of cytokines, increase the ability of scavenging reactive oxygen species, increase the ability of human body to remove bacteria[16], reduce body damage. Therefore, CUR is often used in the treatment of bacterial diseases. Antibiotics have a great cytotoxic effect on normal cells. According to research reports, even the intake of CUR at a high concentration of 12 g/d has almost no side effects on human health[17, 18].

Nanomicelles have become one of the most attractive nanosystems. Micelles can improve drug solubility, reduce side effects and increase drug accumulation by enhancing the retention (EPR) effect and permeability of cell membrane[19]. Polymer micelles, which are self-assembled by hydrophilic and hydrophobic micelles, have been widely used in recent years[20]. Polyurethane micelles self-assembled from amphiphilic polymers have attracted more and more attention in the field of drug delivery due to their distinct advantages including improved solubility of hydrophobic anticancer drugs and prolonged circulation time.[21]. Bacterial cell surface has more negative charges than mammalian cell surface, which is conducive to the preferential electrostatic interaction with positively charged substances. The charge density and hydrophobicity of nanomaterials are important factors for designing

Shaomin Song^{*}, College of Chemistry & Environment, Southwest Minzu University, Chengdu 610041, China

Meihui Yin, College of Chemistry & Environment, Southwest Minzu University, Chengdu 610041, China

Xiaohui Wan, College of Chemistry & Environment, Southwest Minzu University, Chengdu 610041, China

Daoping Yan, College of Chemistry & Environment, Southwest Minzu University, Chengdu 610041, China

Min Yang, College of Chemistry & Environment, Southwest Minzu University, Chengdu 610041, China

Lijiao Yang, College of Chemistry & Environment, Southwest Minzu University, Chengdu 610041, China

Jicong Deng^{*}, Department of Intensive Care, Chengdu Eighth People's Hospital, Chengdu 610041, China. (e-mail: 184930792@qq.com)

[#]Shaomin Song and Meihui Yin contributed equally.

nanomaterials that can selectively destroy bacterial membrane.

In this experiment, we synthesized a multi block polyurethane molecule with polyethylene glycol monomethyl ether (MPEG-DEMA), p-toluenesulfonyl chloride (p-OTs) and CUR. Polyurethane can self assemble into micelles in water. Micelles show positive charge in bacterial environment[22, 23], which enhance the interaction of micelles and bacteria[24]. The successful synthesis of MPEG-CUR-PU was characterized by ¹H NMR, FTIR and UV-Vis. The morphology and structure of MPEG-CUR-PU micelles were characterized by TEM and laser particle size scattering apparatus (DLS)[25].

II. EXPERIMENTAL AND METHODS

A Materials

Polyethylene glycol monomethyl ether (MPEG, Mn=1000), para-toluene sulfonyl chloride (p-OTs), diethanolamine(DEAM), isophorone diisocyanate (IPDI), curcumin (CUR), N,N-Dimethylacetamide (DMAc)

B Synthesis of polyethylene glycol monomethyl ether p-toluenesulfonate (MPEG-OTs)

7.26 g p-toluenesulfonyl chloride (0.04 mol), 20.0 g p-glycol monomethyl ether (Mn = 1000, 0.02 mol) and 3.20 g sodium hydroxide (0.08 mol) respectively, grind them in a mortar for 3 hours, dissolve them in 1000 mL dichloromethane after the reaction, and then use 300 mL sodium hydroxide. The organic phase was collected, dried with anhydrous sodium sulfate, filtered and dried to obtain the white solid product MPEG-OTs.

C Synthesis of polyethylene glycol monomethyl ether diethanolamine (MPEG-DMEA)

80 g of diethanolamine (0.8 mol), 40 g of sodium carbonate (0.4 mol) and 16 g of MPEG-OTs (0.016 mol) were added into a 250 mL round bottom flask. The reaction was carried out overnight at 80°C for 24 h, After the reaction, 200 mL deionized water was added to dissolve, and then 300 mL dichloromethane was used to extract. The organic phase was collected, dried with anhydrous sodium sulfate, filtered and dried to obtain the crude product, which was then gradient eluted and purified by silica gel column (eluent EA: PE=1:10) to obtain the milky solid MPEG-DMEA.

Figure 1. Synthetic route of MPEG-DEAM

D Synthesis of polyurethane MPEG-CUR-PU

First, MPEG-DMEA, IPDI and CUR were added into a three necked flask according to Table 2.1 and protected by nitrogen for 5 minutes. Then, IPDI and 0.1% Sn (Oct)₂ were added at 60°C and polymerized at 80°C for 4 h. A small amount of dry DMAc could be added to control the viscosity. At the end of the reaction, the organic reagents and impurities were removed by stirring at room temperature for 24 h and dropping into deionized water. After drying, the precipitate was dissolved in DCM and the product was purified with ether. The final product was obtained by drying at 40°C atmospheric pressure for 5 h and then at 60°C vacuum for 72 h.

Table 1 Raw material ratio of MPEG-CUR-PU polyurethane

Sample	IPDI / mol	MPEG-DEAM / mol	CUR / mol
MPEG-CUR-PU-1	3	1	2
MPEG-CUR-PU-1.5	3	1.5	1.5
MPEG-CUR-PU-2	3	2	1

E Preparation and characterization of MPEG-CUR-PU micelles

MPEG-CUR-PU micelles were prepared by dialysis. First, 20 mg of polyurethane (mpeg-cur-pu) was completely dissolved in 4 mL of DMAc, and then 15 mL of deionized

water was added drop by drop. After stirring for 4 h, it was transferred to the dialysis bag (MW 500), and the organic solvent was removed by dialysis at room temperature for 72 h. Finally, filter with 0.45 μm pore size syringe and store at 4°C.

The critical micelle (CMC) of polyurethane was determined by using pyrene as fluorescence probe. The

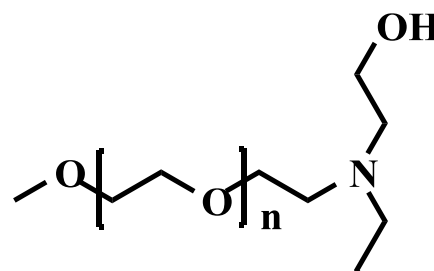


Figure 2. Synthetic route of MPEG-CUR-PU

micelle size and potential laser particle size analyzer (mastersier 2000) were used to measure the CMC. The morphology was detected by transmission electron microscope (TEM) (Fei TECNAI G2 F20).

F Antimicrobial test of polyurethane micelles

MPEG-CUR-PU-1, MPEG-CUR-PU-1.5 and MPEG-CUR-PU-2 micelles were diluted to eleven concentrations by double dilution method and 150 μL micelle solution and 50 μL 10⁶ CFU/mL of *S. aureus* per well added into 96 well plate. The last well was blank control group. After incubation at 37 °C for 18 hours, red tetrazolium was used for color development, and the mic was the lowest inhibitory concentration. The content of CUR in micelles was used as the reference.

III. RESULTS AND DISCUSSION

A. Structure characterization of polyurethane MPEG-CUR-PU

In figure 3, there are two peaks c and d and one a-methyl peak on the benzene ring, and then the two peaks and methyl peak on the benzene ring disappear after being replaced by deam, which indicates that diethanolamine is grafted onto polyethylene glycol monomethyl ether.

In figure 4, the chemical shift of 1.2 ppm is the corresponding peak of methylene in the six membered ring of isophorone diisocyanate, the resonance peak of 1.1 ppm accessory is the proton peak of methyl and methylene linked on the six membered ring of isocyanate; 3.0 ppm is the corresponding peak of -CH-NCO, 3.8 ppm is the proton signal of two O-linked methyl groups in CUR, 3.9 ppm is the characteristic peak of -OCH₃, and 7.2 ppm is the proton signal of benzene ring. The above data are consistent with those reported in CUR. The existence of these peaks proves that IPDI and CUR are grafted into polyurethane segments, and the characteristic peak at 3.7 ppm is the methylene peak of CH₂CH₂O in PEG chain, which proves that peg is contained in the synthesized material.

It can be seen from figure 5 that there is a strong absorption peak at 1050 cm⁻¹, which represents the stretching vibration of C-O of primary alcohol on MPEG-DEMA. 1110 cm⁻¹ corresponds to the stretching vibration of C-O-C and the asymmetric stretching vibration absorption peak at O=C-O, which is 1240 cm⁻¹ Corresponding to the symmetric and asymmetric stretching vibration absorption peaks of O=C-O, the bending vibration peak of N-H is at 1550 cm⁻¹, the infrared absorption of 1740cm⁻¹-1655cm⁻¹ corresponds to the characteristic absorption peak of C=O, and the free -NCO characteristic absorption peak is at 2260-2280 cm⁻¹, It can be seen from the figure that there are weak absorption peaks in this range, indicating the existence of free -NCO in the product. Furthermore, it can be seen that there is a little residue of IPDI in the reactant, and the reaction is not complete. With the increase of mpeg-deam dosage, the intensity of corresponding characteristic absorption peaks also increases. These peaks prove the synthesis of polyurethane, and the stretching vibration peak of CUR

phenol hydroxyl group is at 1511 cm⁻¹, 1650 cm⁻¹-1640 cm⁻¹ is the C-H stretching vibration of CUR on C=C, and the N-H stretching vibration peak or CUR benzene ring skeleton peak is at 3400 cm⁻¹, which indicates that cur has been successfully grafted to the main chain of PU.

Figure 6 shows the change of UV absorption spectrum with the time of natural light irradiation. The UV-Vis Spectrum shows that the UV absorption spectrum changes with the time of natural light irradiation There is a strong characteristic absorption peak near 420 nm, which is the K-band absorption of CUR long chain conjugated system. With the increase of CUR content, the intensity of the absorption peak also increases. The absorption peak at 260 nm is the K-band absorption of benzene ring, which further indicates that CUR is successfully grafted onto polyurethane.

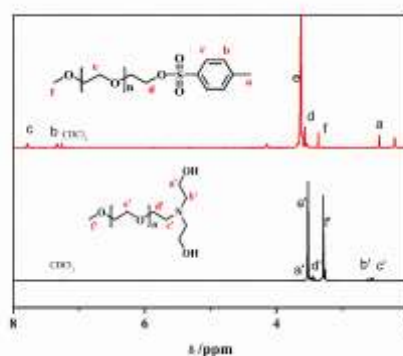


Figure 3. ¹H NMR spectra of MPEG-OTs and MPEG-DEAM in CDCl₃

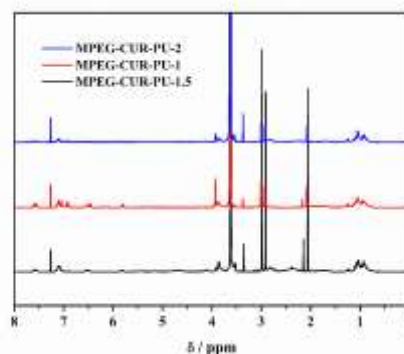


Figure 4. ¹H NMR spectra of MPEG-CUR-PU-1, MPEG-CUR-PU-1.5 and MPEG-CUR-PU-2 in CDCl₃

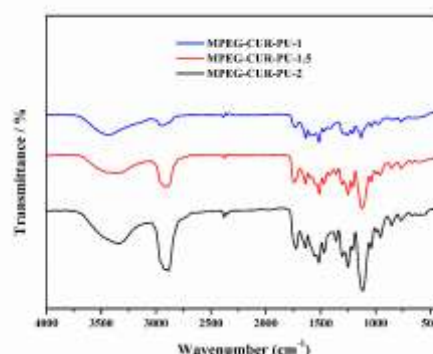


Figure 5. FT-IR spectrum of MPEG-CUR-PU-1, MPEG-CUR-PU-1.5 and MPEG-CUR-PU-2

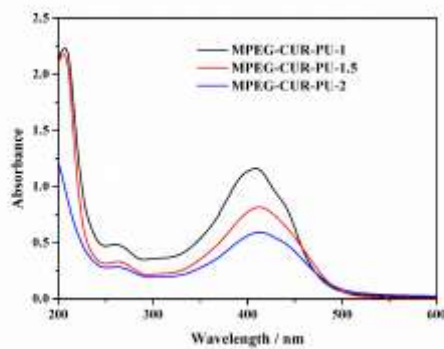


Figure 6. The UV spectra of MPEG-CUR-PU-1, MPEG-CUR-PU-1.5 and MPEG-CUR-PU-2

B. CMC of MPEG-CUR-PU micelles

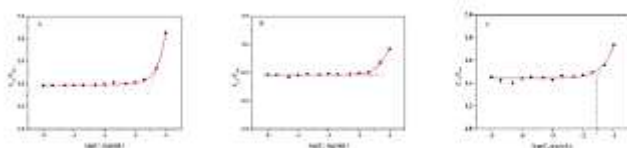


Figure 7. Critical micelle concentrations of MPEG-CUR-PU-1, MPEG-CUR-PU-1.5 and MPEG-CUR-PU-2

This time, the light scattering method is used to determine the CMC of the solution. When the light passes through the solution, part of the light will be scattered by the micelle particles. With the micelle concentration ($\log C$) as the abscissa and the light scattering intensity I_{375}/I_{384} ratio as the ordinate, the intersection of the tangent is the critical micelle concentration, as shown in Figure 7, and the corresponding concentration is the CMC of amphiphilic substances. The measured data are shown in Figure 7, showing the relationship between $\log C$ and I_{375}/I_{384} values of polyurethane micelles with different proportions. A, B and C correspond to polymers MPEG-CUR-PU-1, MPEG-CUR-PU-1.5 and

MPEG-CUR-PU-2 respectively. The concentration corresponding to the point where the slope changes is CMC of the polymer, which is about 0.03162 mg/ml. generally speaking, at the same polymer concentration, the lower CMC, the higher the concentration of the formed aggregate. The lower CMC makes the micelle solution have better dilution stability.

C. DLS and potential characterization of MPEG-CUR-PU micelles

The particle size and distribution of colloid were analyzed by mastersier 2000 laser particle size analyzer. The particle size measurement range is 10 nm-10000 nm, and the scanning speed is 1000 ps. The light source is a highly stable He Ne laser. First, the polymer was dissolved in DMF, and the selective solvent was added to the solution to induce polymer assembly. Then, the co solvent was dialyzed out to obtain mpeg-cur-pu copolymer assembly. Figure 8 is the DLS curve of polyurethane micelles. DLS test shows that the hydrodynamic diameter of the assembly is about 100 nm. The morphology of polyurethane micelles was tested by transmission electron microscope (TEM). The instrument model was JEM-2100 (JEOL Ltd. Japan), and the accelerating voltage was 200 kV. The TEM sample was prepared by dropping a drop of micelle solution with certain concentration on 230 mesh copper mesh, drying at room temperature, and then putting the sample stage into tem for observation. From the TEM diagram of polyurethane micelles (figure 9), it can be seen that the shape of micelles is approximately spherical, the distribution of micelles is uniform, and the particle size distribution is narrow, and the particle size is less than 100 nm. The micelle size of MPEG-CUR-PU-1 is similar to that of TEM (Figure 9).

Table 2 DLS and Zeta of polyurethane micelles

Sample	Diameter / nm	PDI	Zeta Potential / mV
MPEG-CUR-PU-1	108	0.155	0.694
MPEG-CUR-PU-1.5	71.0	0.139	-4.94
MPEG-CUR-PU-2	112	0.162	0.894

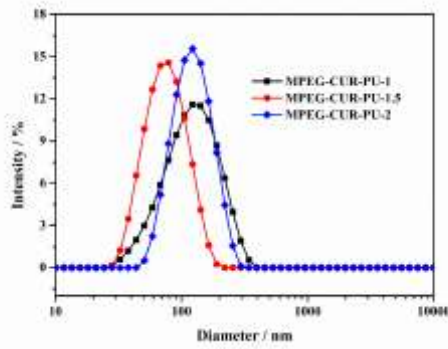


Figure 8. DLS curve of polyurethane micelles

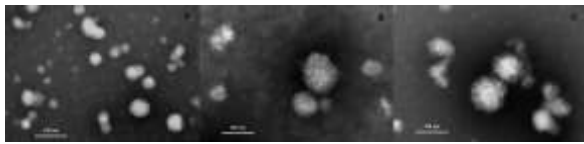


Figure 9. The TEM images of polyurethane micelles MPEG-CUR-PU-1(A), MPEG-CUR-PU-1.5(B) and MPEG-CUR-PU-2(C)

D. Effect of pH value on micelle size

It can be seen from figure 10 that the change of pH value has little effect on the micelle size in acidic environment or when the addition amount of CUR is not greater than MPEG-DEAM. When the addition amount of CUR is increased and the pH value is greater than 6.5, the micelle size of MPEG-CUR-PU-1 increases significantly.

Zeta potential can directly express the state of colloidal particles formed by micelle dispersion in water, and pH value can also directly affect the colloidal particles the aggregation stability of colloidal particles is different under different pH values. It can be seen from figure 10 that when pH value changes from 4.0 to 5.5, MPEG-CUR-PU-1.5 has almost no change. With the increase of pH value, the potential of MPEG-CUR-PU-1 and MPEG-CUR-PU-2 decreases all the time and turns to negative at pH value of 7.0, indicating that the micelles have pH induced surface charge conversion properties. The pH of human normal tissue is 7.4. In the antibacterial drug delivery system, the bacterial infected tissue is usually in acidic environment, so it can be inferred

that the micelle has a relatively stable state in the bacterial infected tissue. Under acidic conditions, the micelles are positively charged by protonation, which improves the ability of penetrating the biofilm. Under physiological conditions (pH = 7.4), the micelles are electronegative, which ensures the long blood circulation of the micelles. It is speculated that in acidic environment, the surface charge of PU micelles may be reversed due to protonation and deprotonation, and some tertiary amine groups will be transferred Therefore, MPEG-CUR-PU micelles have pH induced charge reversal function.

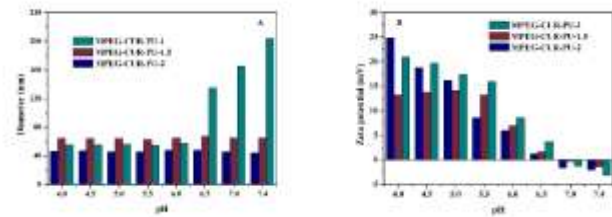


Figure 10. Relationship between pH value and size of polyurethane micelles (A) and relationship between pH value and potential of polyurethane micelles (B)

E. Antibacterial test

When the content of CUR is the same, the higher the content of quaternary ammonium salt in micelles, the better the bactericidal effect of micelles. It can be seen from table 3 that the MIC of MPEG-CUR-PU-1、MPEG-CUR-PU-1.5和MPEG-CUR-PU-2 decrease in turn, indicating that the antibacterial effect increases in turn. This is due to the charge reversal of quaternary ammonium salt in micelles under bacterial acid conditions, which is conducive to the interaction with bacteria with negative surface charge, thus enhancing the germicidal efficacy of CUR.

Table 3 MIC of polyurethane micelles

Sample	<i>S.aureus</i> (ppm)	<i>E.coil</i> (ppm)
MPEG-CUR-PU-1	32.5	36.8
MPEG-CUR-PU-1.5	21.66	24.5
MPEG-CUR-PU-2	14.5	14.5

IV. CONCLUSION

In this study, the polyurethane micelles containing CUR were synthesized by FTIR, ¹H-NMR and UV-Vis. The Antibacterial Polyurethane micelles were characterized by DLS and TEM. The results showed that the prepared micelles were spherical and the average particle size was about 90-100 nm. When the amount of CUR was more than MPEG, zeta potential was negative, It will be helpful to prolong the blood circulation time of micelles.

It can be seen from the relationship between different pH values and micelle size and potential that different amount of CUR has different effects on micelle size and potential, The PEG brush structure on the surface of MPEG-CUR-PU micelles makes the material have charge reversal property. During the micelle self-assembly process, MPEG attached to the hard segment will migrate the DEAM to the micelle surface, showing the surface charge reversal property induced by pH, which is conducive to the realization of targeted antibacterial.

In practical application, the pH value of the environment or the amount of CUR can be adjusted according to the micelle size and potential. This project provides a new way to solve the problem of bacterial infection, but there are still many problems to be solved.

ACKNOWLEDGMENT

This work has been funded by College of Chemistry & Environment, Southwest Minzu University.

REFERENCES

[1] Yao, Y.; Xu, D.; Liu, C.; Guan, Y.; Zhang, J.; Su, Y.; Zhao, L.; Meng, F.; Luo, J., Biodegradable pH-sensitive polyurethane micelles with different polyethylene glycol (PEG) locations for anti-cancer drug carrier applications. *RSC Advances* **2016**, *6* (100), 97684-97693.

[2] Sherrard, L. J.; Tunney, M. M.; Elborn, J. S., Antimicrobial resistance in the respiratory microbiota of people with cystic fibrosis. *The Lancet* **2014**, *384* (9944), 703-713.

[3] Spellberg, B.; Bartlett, J. G.; Gilbert, D. N., The Future of Antibiotics and Resistance. *New England Journal of Medicine* **2013**, *368* (4), 299-302.

[4] Roberts, M., Antibiotic toxicity, interactions and resistance development. *Periodontology 2000* **2002**, *28*, 280-97.

[5] Grimsey, E.; Collis, D. W. P.; Mikut, R.; Hilpert, K., The effect of lipidation and glycosylation on short cationic antimicrobial peptides. *Biochimica et Biophysica Acta (BBA) - Biomembranes* **2020**, *1862* (8), 183195.

[6] Zhang, F.; Yao, H.; Chu, T.; Zhang, G.; Wang, Y.; Yang, Y., A Lanthanide MOF Thin-Film Fixed with Co3O4 Nano-Anchors as a Highly Efficient Luminescent Sensor for Nitrofurantoin Antibiotics. *Chemistry – A European Journal* **2017**, *23* (43), 10293-10300.

[7] Rather, I. A.; Kim, B.-C.; Bajpai, V. K.; Park, Y.-H., Self-medication and antibiotic resistance: Crisis, current challenges, and prevention. *Saudi Journal of Biological Sciences* **2017**, *24* (4), 808-812.

[8] Singer, R. S.; Finch, R.; Wegener, H. C.; Bywater, R.; Walters, J.; Lipsitch, M., Antibiotic resistance—the interplay between antibiotic use in animals and human beings. *The Lancet Infectious Diseases* **2003**, *3* (1), 47-51.

[9] Kocaadam, B.; Şanlıer, N., Curcumin, an active component of turmeric (*Curcuma longa*), and its effects on health. *Critical Reviews in Food Science and Nutrition* **2017**, *57* (13), 2889-2895.

[10] Chainani-Wu, N., Safety and Anti-Inflammatory Activity of Curcumin: A Component of Tumeric (*Curcuma longa*). *The Journal of Alternative and Complementary Medicine* **2003**, *9* (1), 161-168.

[11] Niranjana, A.; Prof, D., Chemical constituents and biological activities of turmeric (*Curcuma longa* L.) -A review. *Journal of Food Science and Technology* **2008**, *45*, 109-116.

[12] Izui, S.; Sekine, S.; Maeda, K.; Kuboniwa, M.; Takada, A.; Amano, A.; Nagata, H., Antibacterial Activity of Curcumin Against Periodontopathic Bacteria. *Journal of Periodontology* **2016**, *87* (1), 83-90.

[13] Sharifi, S.; Fathi, N.; Memar, M. Y.; Hosseiniyan Khatibi, S. M.; Khalilov, R.; Negahdari, R.; Zununi Vahed, S.; Maleki Dizaj, S., Anti-microbial activity of curcumin nanoformulations: New trends and future perspectives. *Phytotherapy Research* **2020**, *34* (8), 1926-1946.

[14] Abdellah, A. M.; Sliem, M. A.; Bakr, M.; Amin, R. M., Green synthesis and biological activity of silver-curcumin nanoconjugates. *Future Medicinal Chemistry* **2018**, *10* (22), 2577-2588.

[15] Teow, S.-Y.; Liew, K.; Ali, S. A.; Khoo, A. S.-B.; Peh, S.-C., Antibacterial Action of Curcumin against *Staphylococcus aureus*: A Brief Review. *Journal of Tropical Medicine* **2016**, *2016*, 2853045.

[16] Kunnumakkara, A. B.; Bordoloi, D.; Padmavathi, G.; Monisha, J.; Roy, N. K.; Prasad, S.; Aggarwal, B. B., Curcumin, the golden nutraceutical: multitargeting for multiple chronic diseases. *British Journal of Pharmacology* **2017**, *174* (11), 1325-1348.

[17] Rafiee, Z.; Nejatian, M.; Daeihamed, M.; Jafari, S. M., Application of curcumin-loaded nanocarriers for food, drug and cosmetic purposes. *Trends in Food Science & Technology* **2019**, *88*, 445-458.

[18] Padmanaban, G.; Rangarajan, P. N., Curcumin as an Adjunct Drug for Infectious Diseases. *Trends in Pharmacological Sciences* **2016**, *37* (1), 1-3.

[19] Yao, Y.; Dai, X.; Tan, Y.; Chen, Y.; Liao, C.; Yang, T.; Chen, Y.; Yu, Y.; Zhang, S., Deep Drug Penetration of Nanodrug Aggregates at Tumor Tissues by Fast Extracellular Drug Release. *Advanced Healthcare Materials* **2021**, *10* (3), 2001430.

[20] Yao, Y.; Xu, D.; Zhu, Y.; Dai, X.; Yu, Y.; Luo, J.; Zhang, S., Dandelion flower-like micelles. *Chemical Science* **2020**, *11* (3), 757-762.

[21] Qiao, Z.; Yao, Y.; Song, S.; Yin, M.; Luo, J., Silver nanoparticles with pH induced surface charge switchable properties for antibacterial and antibiofilm applications. *Journal of Materials Chemistry B* **2019**, *7* (5), 830-840.

[22] Su, Y.; Zhao, L.; Meng, F.; Qiao, Z.; Yao, Y.; Luo, J., Triclosan loaded polyurethane micelles with pH and lipase sensitive properties for antibacterial applications and treatment of biofilms. *Materials Science and Engineering: C* **2018**, *93*, 921-930.

[23] Yao, Y.; Li, C.; Liu, F.; Zhao, P.; Gu, Z.; Zhang, S., Covalent capture of supramolecular species in an aqueous solution of water-miscible small organic molecules. *Physical Chemistry Chemical Physics* **2019**, *21* (20), 10477-10487.

[24] Zhao, L.; Liu, C.; Qiao, Z.; Yao, Y.; Luo, J., Reduction responsive and surface charge switchable polyurethane micelles with acid cleavable crosslinks for intracellular drug delivery. *RSC Advances* **2018**, *8* (32), 17888-17897.

[25] Mun, S.-H.; Jung, D.-K.; Kim, Y.-S.; Kang, O.-H.; Kim, S.-B.; Seo, Y.-S.; Kim, Y.-C.; Lee, D.-S.; Shin, D.-W.; Kweon, K.-T.; Kwon, D.-Y., Synergistic antibacterial effect of curcumin against methicillin-resistant *Staphylococcus aureus*. *Phytomedicine* **2013**, *20* (8), 714-718.